Seasonal discharge response to temperature-driven changes in evaporation and snow processes in the Rhine basin

Joost Buitink[1], Lieke A. Melsen[1], and Adriaan J. Teuling[1]
[1]Hydrology and Quantitative Water Management Group, Wageningen University, Wageningen, Netherlands
Correspondence: Ryan Teuling (ryan.teuling@wur.nl)

Abstract. This study analyses how temperature-driven changes in evaporation and snow processes influence the discharge in the Rhine basin. Using a distributed efficient hydrological model at high spatio-temporal resolution, we separate changes in different forcing components to understand both the separate and combined effects on the discharge in the Rhine basin. By comparing two 10-year periods (1980s and 2010s), we determine the contribution of changes in snow, evaporation and precipitation to changes in discharge. Around half of the observed changes could be explained by the changes induced by snow (10%), evaporation (16%) and precipitation (19%), while 55% was driven by a combination of these variables. Scenarios with increased temperatures show that changes in snow-dynamics can partially offset the fairly constant negative change in discharge induced by evaporation. During spring, however, higher temperatures lead to less meltwater production from the snow packs, further amplifying the reduction in discharge. These results are tested over a range of rooting depths. This study shows how the combined effect of temperature-driven changes affect discharge. With many basins around the world depending on meltwater, correct understanding of these changes is vital.

1 Introduction

Over the last decades, global temperatures have increased considerably (Stocker et al., 2013). The resulting change in climate is generally expected to intensify the hydrological cycle, with more frequent and more severe hydrological extremes (Huntington, 2006). As increased temperatures affect water availability in large river systems in two important ways, it is vital to understand their effects and interactions. Firstly, higher temperatures affect the cryosphere: less precipitation falling as snow and potentially higher snowmelt rates. Surprisingly, Musselman et al. (2017) showed that higher temperatures can even lead to lower snowmelt rates. As snow storages are depleted earlier in the year, it affects the timing of the snowmelt peak in the discharge signal (Jenicek and Ledvinka, 2020; Beniston et al., 2018; Baraer et al., 2012; Huss, 2011; Hidalgo et al., 2009; Collins, 2008; Takala et al., 2009). Since meltwater from "water towers" is vital for billions of people (Immerzeel et al., 2020), it is important have a correct understanding of the expected changes in the cryosphere. Secondly, higher temperatures lead to increased potential evaporation rates, since a warmer atmosphere accommodates higher transport rates (Settele et al., 2015; Wild et al., 2013; Wang et al., 2010). With increased potential evaporation rates, discharge is expected to decrease. Several recent studies have investigated the discharge response to increased temperatures, and generally expect lower discharges resulting from increased evaporation and a shifted seasonality induced by the changed snow dynamics (Milly and Dunne, 2020; Mastrotheodoros et al., 2020; Rottler et al., 2020). However, the relative importance and the combined effect of evaporation and snow processes (including snowfall and -melt, and melt from glaciers) on discharge and its seasonal variability is currently not well understood.

Europe has experienced significant changes in evaporation, snow depth and streamflow over the last decades. For example, Teuling et al. (2019) showed that potential evaporation has increased by about 10% over the period 1960–2010. Their study shows that both changes in precipitation and evaporation had considerable effects on the streamflow. Additionally, a study by Fontrodona Bach et al. (2018) showed that snow depth decreased over the majority of Europe since the 1950s. Europe contains several major river basins with major socio-economic importance. One of these is the Rhine basin, with its headwaters originating from the Alpine region. This basin covers many different types of land cover: from glaciers to lowland areas. Several studies have already investigated the response of this basin under different climate scenarios (e.g., Linde et al., 2010; Hurkmans et al., 2010; Pfister et al., 2004; Shabalova et al., 2003; Middelkoop et al., 2001), and the importance of melt water from snow and ice (Stahl et al., 2016). Yet, none of the studies have investigated the separate and combined response of evaporation and snow processes to rising temperatures.

Spatially distributed modelling becomes increasingly viable, due to the increased computational power, gains in model performance when adding spatial information (Comola et al., 2015; Lobligeois et al., 2014; Ruiz-Villanueva et al., 2012), and increased availability of high resolution data (e.g., Huuskonen et al., 2013; Cornes et al., 2018; Osnabrugge et al., 2017; C3S, 2017). However, the choice of spatial resolution can affect the model parameters (Melsen et al., 2016), and the sign of the simulated anomalies (Buitink et al., 2018). Besides, when finer spatial resolutions are used, the timestep should be reduced as well, as the space and time dimensions are linked (Blöschl and Sivapalan, 1995; Melsen et al., 2016). However, simulations ran at high spatial (and temporal) resolutions usually greatly increase computational demand (for example, the study by Mastrotheodoros et al. (2020) on a 250 m resolution required more than 6×10^5 CPU hours). This not only requires usage of high performance clusters, but also has an undesirable side-effect of increased power consumption (Loft, 2020). There is need for innovative hydrological models which can run on high spatio-temporal resolution without excessive computational demands, such as the recently developed dS2 model (Buitink et al., 2020).

This study investigates the hydrological response to temperature-driven changes in evaporation and snow processes. We test our main hypotheses that both seasonal changes in snow processes and enhanced evaporation will aggravate low flows, and that the changes will increase with temperature under realistic warming. We simulate the Rhine basin at high spatial (4 km) and temporal (1 hour) resolution using a calibrated version of the computationally efficient dS2 model, which is based on the simple dynamical systems approach (Kirchner, 2009; Teuling et al., 2010). The model was run for two decades, and for several scenarios with increased temperatures, to understand both historic changes and expected changes in the future. The simulations performed at this rather unusually high temporal resolution ensures that diurnal variations—vital of evaporation and snow processes—are correctly represented. By separating the temperature-driven effects on evaporation and snow processes, we can understand and quantify the relative importance and interaction of each process.

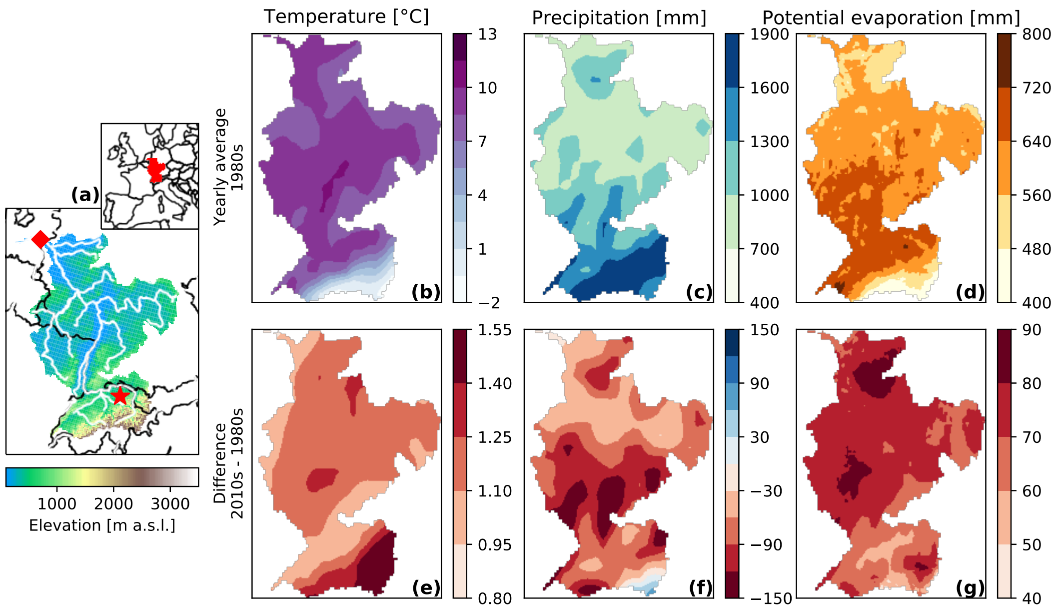

Figure 1. Digital elevation model of the Rhine, and hydro-meteorological changes between the 1980s and the 2010s. Panel a shows the simulation domain, with white lines indicating the main river branches. The red diamond indicates the location of the main outlet, and the red star indicates the location of the Rietholzbach research catchment using for validation. Inset shows the location of the basin within Europe. Top three panels show the yearly average values of the 1980s for temperature, precipitation and potential evaporation (b, c, d, respectively), and bottom three panels (e, f, g) show the differences between the 1980s and the 2010s.

2 Methods

2.1 Study area

This Rhine basin is one of the major basins situated in north-western Europe, covering several countries (see Fig. 1, also for typical climatic values). We focus on the basin upstream of the Netherlands, as this river is of vital importance for the country (e.g. agriculture, shipping). The basin includes part of the Alps, including several glaciers. Despite that this is only a small fraction of the basin (as can be inferred from the digital elevation model in Fig. 1a), it has considerable effects on the discharge (Stahl et al., 2016). As a result, correct understanding of temperature driven changes is important to provide reliable discharge predictions. Despite our focus on this basin, many other river basins depend on meltwater from snow and ice upstream of the basin (Immerzeel et al., 2020). Given differences between hydrological, climatic and geological characteristics, we expect results from this study to give insight into the general hydrological response to higher temperatures.

2.2 Models and data

We used the computationally efficient distributed dS2 model (Buitink et al., 2020) to simulate discharge in the Rhine basin. The model is based on the simple dynamical systems approach (Kirchner, 2009), and is extended with snow and routing modules. As dS2 requires actual evaporation data as input, we ran a soil moisture model (BETA) prior to the rainfall runoff model to simulate the translation from potential evaporation (PET, calculated using the Penman-Monteith equation (Monteith, 1965)) to actual evaporation (AET). Since rootzone depth is an important yet highly uncertain parameter, we included simulations with rootzone depths ranging from 25 to 125 cm, with increments of 25 cm. All simulations are performed at a resolution of 4×4 km and at an hourly time step. The two models are explained in more detail below.

The input data were obtained from the ERA5 reanalysis dataset (C3S, 2017). This dataset is globally available on a $0.25 \times 0.25°$ resolution and at an hourly timestep from 1979 to present. ERA5 data were interpolated to the model grid using bilinear interpolation. We selected two periods with equal length based on the maximum distance between available decades of ERA5 data: 1980-1989 and 2009-2018, referred to as 1980s and 2010s, respectively.

Soil data were obtained from the European Soil Hydraulic Database (EU-SoilHydroGrids ver1.0, Tóth et al., 2017). As this dataset did not contain critical soil moisture content needed by the model to distinguish between water- and energy-limited evaporation regimes (Denissen et al., 2020), it was determined as the mean between wilting point and field capacity. The hygroscopic moisture content was calculated from the moisture retention curve based on Mualem-van Genuchten parameters at -10 MPa (Laio et al., 2001; Tóth et al., 2017). The clay content of the European Soil Hydraulic Database was used to calculate the pore size distribution (b) through a linear fit of the values found in Clapp and Hornberger (1978). For the depth of the rootzone, we chose a depth of 75 cm, but also included simulations ranging from 25 to 125 cm with increments of 25 cm, to account for the uncertainty of this parameter. The potential evaporation input data was calculated using the Penman-Monteith equation (Monteith, 1965), based on ERA5 input data.

2.2.1 BETA

A simple soil moisture model (BETA, Beta EvapoTranspiration Adjustment) is used to preprocess the evaporation input. This model simulates the rootzone, and determines evaporation reduction based on the amount of water stored in the rootzone. Actual evaporation is assumed to be a function of the available soil moisture such that:

$$ET_{\mathrm{actual}} = ET_{\mathrm{potential}} \cdot \beta(\theta), \tag{1}$$

where β represents the evaporation reduction parameter as a function of soil moisture θ. β is defined using three linear relations with θ, based on Laio et al. (2001):

$$\beta(\theta) = \begin{cases} \beta_{\mathrm{w}} \frac{\theta - \theta_{\mathrm{h}}}{\theta_{\mathrm{w}} - \theta_{\mathrm{h}}} & \text{if } \theta \leq \theta_{\mathrm{w}} \\ \beta_{\mathrm{w}} + (1 - \beta_{\mathrm{w}}) \frac{\theta - \theta_{\mathrm{w}}}{\theta_{\mathrm{c}} - \theta_{\mathrm{w}}} & \text{if } \theta_{\mathrm{w}} \leq \theta \leq \theta_{\mathrm{c}} \\ 1 & \text{if } \theta_{\mathrm{c}} \leq \theta \leq \theta_{\mathrm{s}} \end{cases} \tag{2}$$

where β_w represents the evaporation reduction factor at wilting point (set to 0.1), θ_h represents the hydroscopic point, θ_w the wilting point, θ_c the critical soil moisture content, and θ_s the saturated soil moisture content.

Leakage from the rootzone is calculated to simulate the vertical movement of water. This water is assumed to be gone from the rootzone, as we do not simulate a layer below the rootzone. The leakage is based on the unit-gradient assumption in combination with the Clapp and Hornberger (1978) model for unsaturated conductivity, integrated over a timestep Δt:

$$Q_\mathrm{leakage} = L\theta_\mathrm{t} - L\theta_\mathrm{s}\left[\left(\frac{\theta_\mathrm{t}}{\theta_\mathrm{s}}\right)^{-2b-2} + \frac{(2b+2)k_\mathrm{s}\Delta t}{\theta_\mathrm{s}L}\right]^{-\frac{1}{2b+2}}, \tag{3}$$

where L represents the depth of the rootzone, θ_t the soil moisture content at timestep t, b the pore size distribution, and k_s the saturated conductivity. The value for b is calculated through the clay fraction (CF), using a linear fit based on the values in Clapp and Hornberger (1978):

$$b = 13.52 \cdot \mathrm{CF} + 3.53. \tag{4}$$

Finally, the water balance for the rootzone is defined as follows:

$$\theta_{\mathrm{t}+1} = \theta_\mathrm{t} + \Delta t(P_\mathrm{rain} + M_\mathrm{snow} - ET_\mathrm{actual} - Q_\mathrm{leakage}), \tag{5}$$

where P_rain is the rate of rainfall at timestep t, M_snow the rate of snowmelt at timestep t, both are inferred the same way as in the dS2 model (Buitink et al., 2020).

2.2.2 dS2

A conceptual rainfall-runoff model is used to simulate the discharge in the Rhine basin. The dS2 model (Buitink et al., 2020) is based on the simple dynamical systems approach, as proposed by Kirchner (2009). This approach is based on the assumption that discharge is a function of storage, such that changes in storage can be related to changes in discharge via a discharge sensitivity function:

$$Q = f(S), \tag{6}$$

$$\frac{\mathrm{d}Q}{\mathrm{d}t} = \frac{\mathrm{d}Q}{\mathrm{d}S}\frac{\mathrm{d}S}{\mathrm{d}t} = \frac{\mathrm{d}Q}{\mathrm{d}S}(P - ET - Q), \tag{7}$$

where Q represents the discharge, S the storage, P and ET the precipitation and actual evaporation, respectively, and $\frac{\mathrm{d}Q}{\mathrm{d}S}$ represent the discharge sensitivity to changes in storage, referred to as $g(Q)$. This concept has been successfully applied and validated in several catchments across Europe (Kirchner, 2009; Teuling et al., 2010; Krier et al., 2012; Brauer et al., 2013; Melsen et al., 2014; Adamovic et al., 2015). Buitink et al. (2020) further developed the concept so it can be applied in a distributed way, to allow the simulation of larger catchments, while respecting the original scale of development. A new equation to better capture the typical shape of the g(Q) relation is proposed by Buitink et al. (2020), which contains three parameters:

$$g(Q) = e^{\alpha+\beta\ln(Q)+\gamma/Q}. \tag{8}$$

Additionally, the model has been extended with a snow module based on Teuling et al. (2010), and a routing module based on the width function (Kirkby, 1976). The snow module is a degree-day method, with separate melt factors for snow and glaciers.

To calibrate dS2, we optimized the three discharge sensitivity parameters, the degree day factor for both snow and glacier pixels, and an evaporation correction factor. The evaporation correction factor is included to correct any bias errors in the forcing data. According to Boussinesq's theory of sloping aquifers (Rupp and Selker, 2006) and the results found in Karlsen et al. (2019), systems with higher slopes are expected to show higher discharge sensitivity values. Therefore, the discharge-sensitivity parameters were defined as a linear function of the slope of each pixel, based on the hypothesis that regions with steeper slopes show a more responsive storage-discharge relation than regions with gentle slopes. This resulted in two fitting parameters (slope and intersect) for each of the three discharge sensitivity parameters. Latin Hypercube sampling was used to gain parameter values evenly sampled across the possible parameter space. The period 2004–2008 was used for calibration. To ensure realistic model performance across the entire basin, the Kling-Gupta efficiency (KGE, Kling and Gupta, 2009) score was calculated at 13 discharge measurement stations within the Rhine basin (see supplement for corresponding locations and performance metrics). KGE values across all stations are averaged, and the parameters from the run with the best average KGE are selected. The resulting parameter values can be found in the supplement.

2.3 Experimental setup

We have split our analysis in two parts. Firstly, we compare two decades to understand the relative impact of each forcing variable. Secondly, we increase temperature values with 0.5 degree increments to understand how an increase in temperature affects the hydrological response in the Rhine basin. We explain both experiments in more details below.

2.3.1 Forcing swap

In the first experiment, we aim to understand how each forcing variable can explain the resulting changes in discharge, and their relative importance. To perform this, we setup the experiment according to the conceptual overview presented in Fig. 2. The first two simulations are straightforward: using all forcing variables from either the 1980s or the 2010s to produce the corresponding discharge timeseries ("1980s" and "2010s"). In order to investigate how temperature influences evapotranspiration and snow processes separately, we perform model runs in which the total temperature change is separated into temperature effects on evapotranspiration ("Changed $\mathrm{T_{evap}}$") and snow processes ("Changed $\mathrm{T_{snow}}$"). In addition, another run is performed with only changes in P ("Changed P"), so that these individual runs can be compared to a run where all changes in forcing are enabled ("2010s"). The resulting simulated discharge is compared to the 1980s run, to determine the discharge change. In this way, we can evaluate the relative impact of each forcing variable on the discharge.

We sum the discharge changes of the three forcing swapped runs, to obtain $\mathrm{Sum}\Delta$ (as timeseries):

$$\mathrm{Sum}\Delta = \Delta\mathrm{Q_P} + \Delta\mathrm{Q_{T\ snow}} + \Delta\mathrm{Q_{T\ evap}} \tag{9}$$

where $\Delta\mathrm{Q_x}$ represents the discharge difference of the forcing swapped simulations. We can use this $\mathrm{Sum}\Delta$ to study how well it explains the 2010s run, by comparing it to $\Delta\mathrm{Q_{2010s}}$. We hypothesise that when $\mathrm{Sum}\Delta$ is equal to $\Delta\mathrm{Q_{2010s}}$, the effect of the

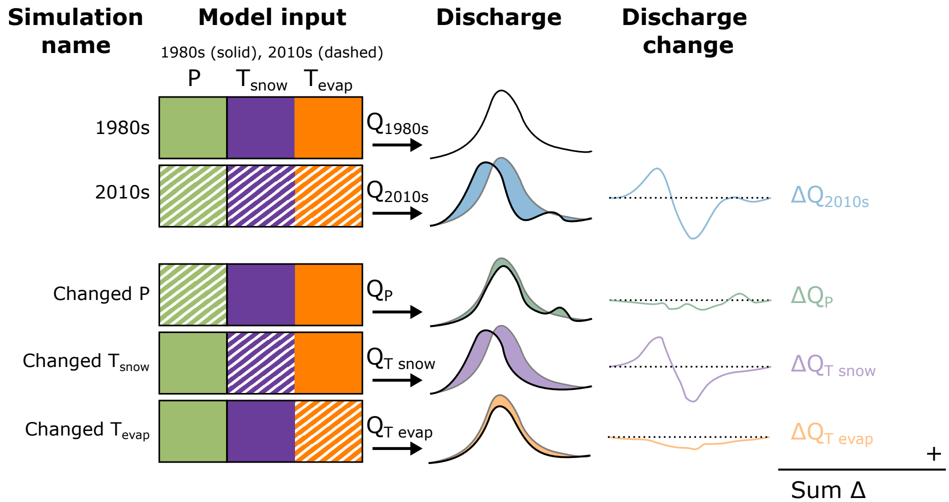

Figure 2. Conceptualization of the forcing swap experiment, showing the different simulations (rows) and steps in the analysis (columns). The different forcing variables are visualized as colored blocks, where the solid and dashed boxes indicate forcing data from the 1980s and the 2010s, respectively.

forcing is additive, and together explain all differences. We will refer to this as the direct effects. In the case of a discrepancy between $\mathrm{Sum}\Delta$ and $\Delta\mathrm{Q}_{2010\mathrm{s}}$, this can be attributed to interaction between the three forcing components. We will refer to this as indirect effects. We define $\mathrm{Sum}\Delta$ to have explanatory value when it has the same sign as $\Delta\mathrm{Q}_{2010\mathrm{s}}$. We calculate the contribution of the direct effects (ϕ) using the following equation:

$$\phi = \begin{cases} \frac{\min(\mathrm{Sum}\Delta, \Delta\mathrm{Q}_{\mathrm{all}})}{\max(\mathrm{Sum}\Delta, \Delta\mathrm{Q}_{\mathrm{all}})}, & \text{if } \mathrm{sign}(\mathrm{Sum}\Delta) = \mathrm{sign}(\Delta\mathrm{Q}_{\mathrm{all}}) \\ 0, & \text{if } \mathrm{sign}(\mathrm{Sum}\Delta) \neq \mathrm{sign}(\Delta\mathrm{Q}_{\mathrm{all}}) \end{cases} \tag{10}$$

This value can then be used to calculate the relative (direct) contribution of each forcing variable, using the following equation:

$$\phi_{\mathrm{x}} = \frac{\mathrm{abs}(\Delta\mathrm{Q}_{\mathrm{x}})}{(\mathrm{abs}(\Delta\mathrm{Q}_{\mathrm{P}}) + \mathrm{abs}(\Delta\mathrm{Q}_{\mathrm{T\ snow}}) + \mathrm{abs}(\Delta\mathrm{Q}_{\mathrm{T\ evap}}))} \cdot \phi \tag{11}$$

where $\Delta\mathrm{Q}_{\mathrm{x}}$ should be replaced by $\Delta\mathrm{Q}_{\mathrm{P}}$, $\Delta\mathrm{Q}_{\mathrm{T\ snow}}$, or $\Delta\mathrm{Q}_{\mathrm{T\ evap}}$.

2.3.2 Increased temperatures

In the second experiment, we raise temperature with 0.5°C increments to understand how the basin responds to higher temperatures. We use the 1980s period as baseline, and increase the temperature until 2.5°C, to match realistic temperature projections. By separating the effects of temperature on evaporation and snow processes, we can understand their relative importance for each temperature increase.

3 Results

3.1 Forcing comparison and validation

A first comparison of average temperature, precipitation and potential evaporation reveals considerable differences between the two periods (Fig. 1). Over the entire Rhine basin, yearly average temperature has increased with more than 1° C, from 8.1° C to 9.3° C between 1980s and 2010s. Largest differences are found in the eastern Alps, where average temperature has risen by 1.5° C (Fig. 1b, e). Average precipitation is lower in the 2010s over the majority of the Rhine basin, with the yearly average precipitation sums decreasing from 1146 mm to 1066 mm (Fig. 1c, f). Spatial differences in precipitation are, however, less homogeneous over the basin than the changes in temperature and potential evaporation. As a result of the increased temperatures, average potential evaporation also substantially increased from 607 mm to 678 mm from the 1980s to the 2010s, with the largest increases occurring in the northern parts of the basin (Fig. 1d, g).

A thorough validation is required in order to ensure that models simulate the correct sign and magnitude of the trends (Melsen et al., 2018). Therefore, we validated dS2 on multiple levels: discharge of the total catchment, and snow and evaporation dynamics at both local and basin scale. Discharge validation (Fig. 3a) shows that dS2 simulates the discharge with high KGE values in both periods. Panel b shows how the average discharge differs between the two periods, with lower discharges in the 2010s for the majority of the year. Discharge during the 2010s does not show as high discharge values in June, and shows lower discharge values occurring later in the year. Kling-Gupta efficiencies for each period and several stations within the basin can be found in the supplementary information (Table S1).

Additionally, validation of snow and evaporation is performed at two levels: local temporal validation with point observations from the Rietholzbach research catchment in Switzerland (Seneviratne et al., 2012) (Fig. 4a and d), and spatial validation of evaporation and snow patterns using GLEAM (v3.3, Martens et al., 2017) and European Climate Assessment & Data Set (ECA&D, Tank et al., 2002; Fontrodona Bach et al., 2018) (Fig. 4b, c, e, and f).

For the validation with data from the Rietholzbach catchment, we compare simulated actual evaporation with observed evaporation from a lysimeter, and compare simulated snow storage with observed snow height measurements in Fig. 4. Due to data availability limitations, we had to resort to our calibration period. Since dS2 was only calibrated on discharge, this still can be interpreted as validation. Both variables are correctly represented, and show similar variability as the observations, even at hourly timescale. The simulated evaporation generally shows a smoother signal than the observations. However, the simulated evaporation is based on relatively coarse ERA5 data, which could cause the lack of small scale variability. Snow storage shows a very similar pattern. It has to be noted that snow height observations cannot be directly converted into snow water equivalent, due to e.g. compaction. Yet, dS2 simulates melt and snowfall at moments corresponding with observations, as is confirmed by the contingency table in panel b. Given that dS2 is not calibrated on these variables, and the difference in spatial scale of the input data, this shows that dS2 is able to correctly simulate evaporation and snow processes.

This is confirmed in the spatial validation, where we compare the actual evaporation results from the BETA model with results from GLEAM (Martens et al., 2017). It should be noted that this is not a true validation, since GLEAM is not a completely independent observational dataset. Despite this, GLEAM is often considered as a reference for spatio-temporal validation of

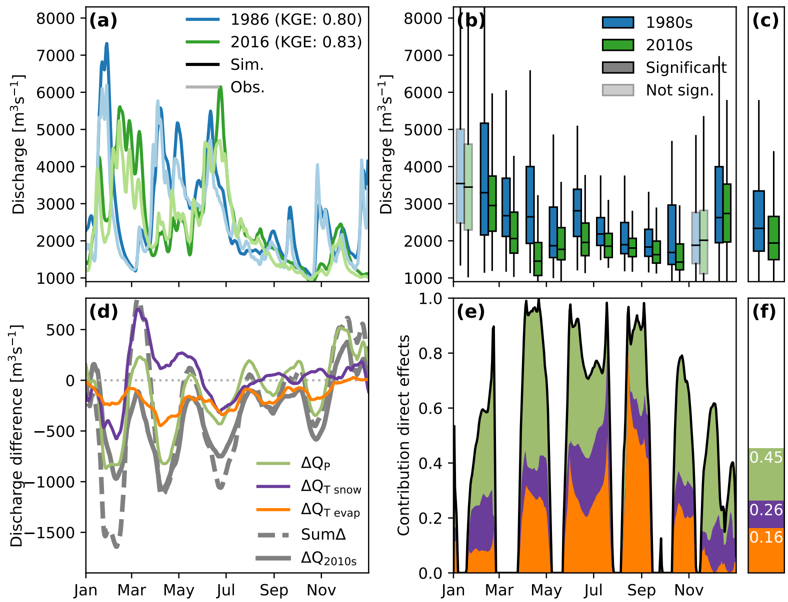

Figure 3. Attribution of discharge changes between the 1980s and the 2010s. Panel a compares simulated (dark colored) with observed (light colored) discharge values for one representative year in each period. Panel b and c compare the monthly and yearly (respectively) simulated discharge values between the two periods, where full coloured boxes are significantly different ($p<0.05$). Panel d shows the difference of model simulations where one of the forcing data has been swapped with the time series from the 2010s. Panel e shows the contribution of direct effects (black line), and the contribution of each forcing variable, to the total change between the two periods. Overall mean values of the timeseries in panel e are presented in panel f.

ET. Additionally, BETA uses a single rooting depth value for the Rhine basin. We see some deviations in terms of magnitude, where BETA simulates slightly higher values than GLEAM. However, despite the differences in spatial resolution, the patterns are well represented in BETA: higher values in the southern region of the basin, with lower values in the middle/northern regions. The simulated snow storage is compared with observations from the ECA&D dataset, provided by Fontrodona Bach et al. (2018). It should be noted that the observations are measured as snow height, while dS2 simulates snow water equivalent. This dataset only contains point observations, and no stations in France are available. Despite this, dS2 simulates snow cover with a similar pattern as is observed: with high values in the Alps and southeastern region, and low values in the middle and northern parts of the basin.

3.2 Forcing swap

Investigating the differences between the “forcing-swapped” runs gives insight on how each variable affects the discharge (see Fig. 3d, e, and f). Changing the precipitation ($\Delta \mathrm{Q_P}$) has substantial effects on the discharge (Fig. 3d), swinging from large negative discharge differences to positive differences. This is not unexpected, as precipitation is the factor controlling water input into the basin. Changing only the temperature affecting snow processes ($\Delta \mathrm{Q_{Tsnow}}$) shows discharge differences mostly

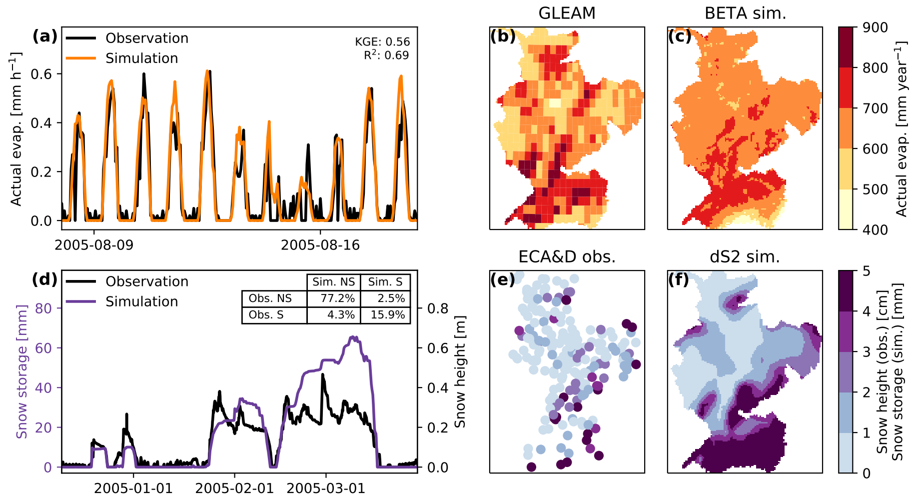

Figure 4. Temporal and spatial validation of evaporation rates (a, b, c) and snow storage (d, e, f). Panels a and d show validation with observations from the Rietholzbach research catchment (location can be found in Fig. 1a), with the table in panel d showing the contingency table with the percentage of occurrences with snow (S) and with no snow (NS). Note that panel d has two y axes: snow storage for the simulation and snow height for the observations. Panels b and c show the annual mean actual evaporation of 2005 as determined with both GLEAM and BETA (with a rooting depth of 75 cm). Panels e and f show annual mean snow heights of 2005, as observed in the ECA&D dataset (snow height), and simulated with dS2 (snow storage).

in the first half of the year. The reduction of discharge in January and February is caused by overall higher temperatures: less snow has fallen in the preceding months, leading to less snowmelt in January and February. From March to May, this simulation shows higher discharge values resulting from enhanced melt from snow and ice. From July onwards, discharge values converge back to the original 1980s simulation, indicating that the discharge regime becomes less snow dominated. The simulation with evaporation from the 2010s ($\Delta \mathrm{Q}_{\mathrm{Tevap}}$) shows a discharge reduction over the entire year. The higher PET leads to higher actual evaporation, decreasing the discharge.

The contribution of direct effects in Fig. 3e-f gives an indication on the amount of interaction between the three forcing variables. Values close to 1 indicate that there is little interaction, as the sum of the differences is able to explain all changes. The contribution of direct effects is lowest during March and around October. During these periods, the storage conditions of the basin largely control the discharge response, either through snow storage or water available to generate runoff. In spring, changes in the available snow storage are the result of interactions between temperature and precipitation. In summer, discharge is controlled by water that is available for runoff generation, which is controlled by interactions of precipitation and evaporation. These interactions of forcing variables cannot be captured by simply combining the individual discharge responses, hence the relatively large contribution of indirect forcing effects during these periods. Panel f shows that, overall, it is possible to explain almost half of the 2010s discharge scenario. The temperature effects of evaporation and snow (0.16 and 0.10, respectively, totalling to 0.26) are just as important as the changes induced by differences in precipitation (0.19), yet due to the large role of interactions, no more than 45% can be explained using this simple addition.

3.3 Increased temperatures

In the second experiment, we investigate the role of temperature increases on changes in discharge. Higher temperatures affect the hydrological cycle either through evaporation, snow processes, or a combined effect of the two. Using the dS2 model, separate simulations of temperature effects on evaporation ($\mathrm{Q_{Tevap}}$), snow ($\mathrm{Q_{Tsnow}}$) and their combined effect ($\mathrm{Q_{Tboth}}$) allow us to understand which variable is causing the main changes. These time series are presented in Fig. 5a, including the 1980s run as reference. Three periods are highlighted, which represent typical discharge regimes: high discharge during January and February, the meltwater peak during May and June, and low discharge during September and October. For each of these periods, the change in discharge shows a roughly linear relation with temperature increase. This is in line with our hypothesis, that higher temperatures will lead to larger differences in discharges. The resulting near-linear relation is interesting, as both snow and evaporation processes are threshold processes. We expect to see a more non-linear response to temperature when reaching more hydrological extremes.

Surprisingly, for the during January-February and September-October (panel b and d), the modified snow run shows behaviour opposite to both the modified evaporation run and the combined run. In these cases, the increased discharge as result of a change in snow processes can partially offset the negative discharge change induced by the increased evaporation. This ensures that the combined change in discharge is less severe than when only the change in evaporation is considered. However, during May-June, both evaporation and snow processes show a negative discharge change, enhancing the combined change in discharge. As a result, the discharge of the combined run shows an even larger reduction in discharge, where even the peak during June from the 1980s has been largely diminished (see panel a). Substantial influence of rooting depth on the evaporation simulation is visible, yet the trend direction with increasing temperatures remains equal. Shallower rooting depth values induce more soil moisture stress since less water is available, leading to higher discharges.

To understand the cause of these changes, the change in generated runoff per model pixel is shown in Fig. 6a. This figure shows that the majority of the basin produces less runoff for all three periods. Only the southern regions of the basin show a different response. During January and February, these regions produced more runoff, resulting from the increased snowmelt and increased liquid precipitation. In the other periods, only a few pixels produced more runoff. These pixels correspond to the glaciers in the Alps, which produced more meltwater resulting from the increased temperatures, and explain the positive discharge change in Fig. 6d.

By separating the effects of evaporation, snow and their combined effect, we can understand the relative importance of the interplay of these variables. In Fig. 6b, the fraction of the basin that is dominated by one of these three options is plotted against the relative change in mean discharge for each period. As expected, the majority of the basin is controlled by the change induced by a change in evaporation (84–94%). As a result, the mean discharge is reduced by $\pm 17\%$. Contrasting, a limited fraction of the basin (1–6%) is dominated by the change induced by snow, yet still has a considerable effect on the mean discharge: varying between -3% and 6%. Pixels in the basin where a combination of changed induced by snow and evaporation

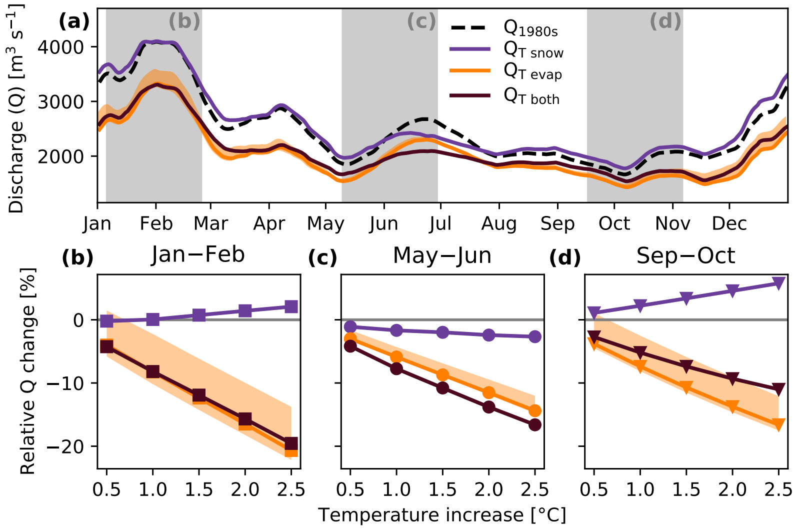

Figure 5. Discharge sensitivity to temperature increase. Panel a shows the yearly average discharge under a 2.5°C increase, and panel b shows changes during typical discharge events with stepwise temperature increases. Typical discharge periods highlighted in panel a match the periods used to compare the mean discharges in panels b, c, and d. Shaded orange areas indicate the uncertainty induced by effective rooting depth (25-125 mm), where higher discharges match shallower depths and vice versa.

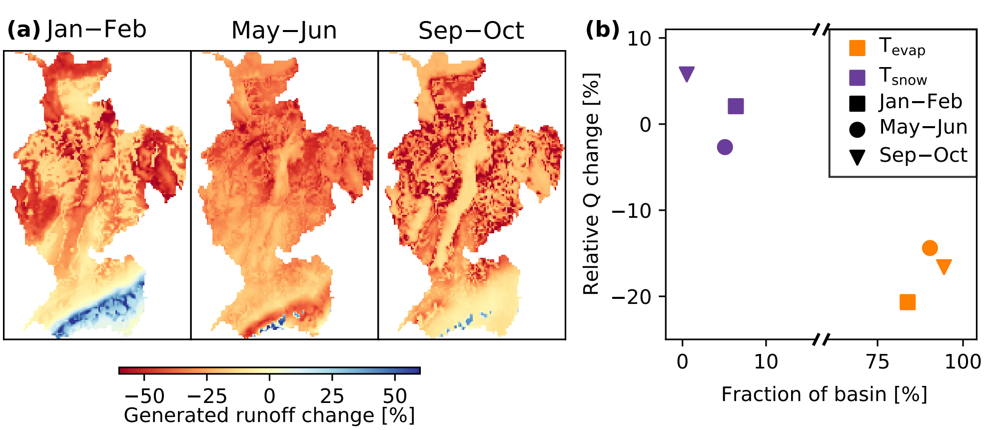

Figure 6. Spatial differences in the Rhine basin under the +2.5°C scenario. Panel a shows the differences in generated runoff for the three periods highlighted in 5a. Panel b shows the fraction of the basin where 80% of the changes could be explained by either evaporation or snowmelt, and the average discharge change corresponding to each process.

are required, take only a very small fraction of the basin (<1%). Generally, these regions are at the transition between snow dominated and evaporation dominated regions. Overall, the change induced by T_{snow}—despite the small contributing area—substantially affects the discharge. More details on the response for each temperature increase can be found in the supplement.

4 Discussion

We compared two periods of 10 years to investigate the relative importance of changes in temperature, evaporation and precipitation. Over these periods of 10 years, most interannual variability is averaged out, allowing us to objectively investigate the effect of different temperatures on the hydrological response. Furthermore, the choice of spatial model resolution is a balance between data availability, computational time and underlying modelling concept. Here we selected a resolution of 4×4 km, so we can use the ERA5 forcing data with bilinear resampling (without adding more degrees of freedom, uncertainty, and potential errors), have short runtimes (simulating 10 years including all I/O operations takes just over 5 minutes on a normal desktop), and apply the model at it's proven spatio-temporal scale (± 10 km^2 at hourly timestep). Contrasting, the study by Mastrotheodoros et al. (2020) used a much finer spatial resolution, but at the cost of enormous CPU times.

Several other recent studies have investigated the hydrological response to increased temperatures via either changes in evaporation and/or snow processes. Below, we compare our results with the results found in three of these studies. Firstly, the study by Rottler et al. (2020) showed a decrease in runoff seasonality in rivers fed by melt water from snow, over the period 1869–2016. They found higher discharges during winter and spring, and lower discharges during summer and autumn. The authors conclude that reservoir constructions in these snow-dominated rivers is likely to cause this redistribution of discharge. However, our temperature experiment shows a similar change in discharge: with higher discharges in winter and spring, and lower discharges during summer. As the dS2 model does not include dams and other reservoirs, this signal can be attributed to a change in discharge production. Secondly, a recent study investigating the response of several basins in Czechia to changes in snowmelt, concluded that snowmelt started earlier in the year, which also reduced summer low flows via baseflow (Jenicek and Ledvinka, 2020). However, our study shows that low flows during September/October in the Rhine are slightly increased as a result of changes in snow processes. This can be explained by that fact that the Rhine basin includes glaciers, which produce more meltwater with higher temperatures (assuming the glacier is thick enough to facilitate this melt). This increase in meltwater resulted in higher discharge volumes during summer. Thirdly, Milly and Dunne (2020) showed a reduction of discharge in the Colorado river basin, and conclude that this is driven by increased evaporation. This increase of evaporation is attributed to a reduction in snow cover, and hence a decreased albedo. Despite the different basin, our study supports the conclusion that increased temperatures reduce discharge through both changes in snow processes, and increased evaporation. Our model does not account for changes in albedo, but does allow areas previously covered in snow to evaporate water. And while differences in climate zone of the Colorado and Rhine basins make it challenging to compare the absolute numbers, the sign of the trend is equal.

Musselman et al. (2017) concluded a lowering of snowmelt rates due to a shift of the melt season towards a period with lower available energy (spring in stead of summer). They simulated the snowpack with a more complex energy balance, rather than our degree-day method. The dS2 model does not include the radiation driven changes, but does simulate that snowmelt occurs earlier in the year. This means that, under increased temperature scenarios, snowmelt occurs on days where previously no melt was possible. It is highly probable that on these days, the maximum temperature is lower than it would have been without a temperature increase. This results in lower snowmelt rates. Additionally, dS2 does simulate earlier depletion of the snowpack, which also reduces snowmelt rates. Despite our different aim and approach, we believe that our study supports the findings of Musselman et al. (2017).

When comparing our results with results from studies perform in the Rhine basin (e.g., Linde et al., 2010; Hurkmans et al., 2010; Pfister et al., 2004; Shabalova et al., 2003; Middelkoop et al., 2001), we see similar results. These studies focussed mainly on understanding and/or projecting the Rhine discharge under climate scenarios. Yet all these studies agree that the snowmelt peak will occur earlier in the year, and that the basin is expected to transition from a mixed rain/snow-fed river to a mostly rain-fed river. Additionally, all studies agree to expect higher evaporation rates, further reducing the discharge. This is all in line with our study, despite the fact that we did not investigate changes in precipitation in our temperature scenarios. Furthermore, the Rhine basin contains several hydraulic control measures, which are currently not represented in our model structure. Despite this, we still reach good model performance, suggesting that these structures currently do not have a very large influence on the discharge dynamics at the basin outlet. In the future, however, the management schemes and number of structures can be altered to accommodate the changes in the hydrological cycle. As these changes are a large unknown, we decided to only focus on the natural hydrological response.

5 Conclusions

Temperature, evaporation and precipitation substantially changed from the 1980s to the 2010s in the Rhine basin, reflecting changes that are typical for many larger basins around the world. In the 2010s, basin average temperature was more than 1°C higher, potential evaporation was almost 70 mm higher, and precipitation decreased with 80 mm. Discharge between these two periods was significantly different for 10 out of 12 months. Each individual forcing variable can partly explain these discharge differences: 10% can be explained by the changed snowfall and melt dynamics, 16% is explained by the changed evaporation, 19% by the changed precipitation; leaving 55% to be explained by the interaction of these variables. Higher temperatures overall reduce the discharge. However, snow processes (snowfall and melt from snow and glaciers) can partially offset the negative change in discharge during the lowflows in September-November, which was contrary to our expectations. The discharge response during May-July matches our hypothesis that both changes in snow processes and evaporation enhance the reduction in discharge. Less than 10% of the basin is dominated by the changed snow dynamics, yet it changes the discharge with as much as 6%, depending on the season.

This study focusses on the Rhine basin, yet these results can provide insight for the many different basins around the globe, which also depend on both rain- and snowfall. With higher temperatures, changes in snow processes can partially offset the discharge reduction from enhanced evaporation over the majority of the year. However, the season where runoff generation is reduced due to smaller snow storages (and potentially smaller glaciers) should be identified in each basin, as this part of the year is impacted the most. Many regions rely on “water towers” for their year-round water availability (Immerzeel et al., 2020), where the mountainous regions cover varying fractions of the basin. In many basins, more of the discharge originates from these water towers than in the Rhine basin, amplifying our results. Here, higher temperatures would likely imply even stronger negative amplitudes in discharge trends during the melt season. Enhanced melt can partially offset the negative change in discharge caused by the increased evaporation, but can enhance the negative change when snow storages are eventually depleted earlier in the year.

Code and data availability. Model code and information is available at Buitink et al. (2020). Forcing data was obtained from C3S (2017). Soil data was obtained from Tóth et al. (2017).

Author contributions. JB and AJT designed the study. JB performed the model simulations and analyses, and wrote the manuscript with contributions from LAM and AJT.

Competing interests. The authors declare that they have no conflict of interest.

Acknowledgements. We would like to thank Christoph Brühl and Doke Schoonhoven for their work during their MSc. thesis, which set the foundation for this study.

References

Adamovic, M., Braud, I., Branger, F., and Kirchner, J. W.: Assessing the simple dynamical systems approach in a Mediterranean context: application to the Ardèche catchment (France), Hydrology and Earth System Sciences, 19, 2427–2449, https://doi.org/https://doi.org/10.5194/hess-19-2427-2015, https://www.hydrol-earth-syst-sci.net/19/2427/2015/, 2015.

Baraer, M., Mark, B. G., McKenzie, J. M., Condom, T., Bury, J., Huh, K.-I., Portocarrero, C., Gómez, J., and Rathay, S.: Glacier recession and water resources in Peru's Cordillera Blanca, Journal of Glaciology, 58, 134–150, https://doi.org/10.3189/2012JoG11J186, https://www.cambridge.org/core/journals/journal-of-glaciology/article/glacier-recession-and-water-resources-in-perus-cordillera-blanca/5CEA7495D2BF050058A6B7280FE89A12/core-reader, publisher: Cambridge University Press, 2012.

Beniston, M., Farinotti, D., Stoffel, M., Andreassen, L. M., Coppola, E., Eckert, N., Fantini, A., Giacona, F., Hauck, C., Huss, M., Huwald, H., Lehning, M., López-Moreno, J.-I., Magnusson, J., Marty, C., Morán-Tejéda, E., Morin, S., Naaim, M., Provenzale, A., Rabatel, A., Six, D., Stötter, J., Strasser, U., Terzago, S., and Vincent, C.: The European mountain cryosphere: a review of its current state, trends, and future challenges, The Cryosphere, 12, 759–794, https://doi.org/https://doi.org/10.5194/tc-12-759-2018, https://www.the-cryosphere.net/12/759/2018/, 2018.

Blöschl, G. and Sivapalan, M.: Scale issues in hydrological modelling: A review, Hydrological Processes, 9, 251–290, https://doi.org/10.1002/hyp.3360090305, http://onlinelibrary.wiley.com/doi/10.1002/hyp.3360090305/abstract, 1995.

Brauer, C. C., Teuling, A. J., Torfs, P. J. J. F., and Uijlenhoet, R.: Investigating storage-discharge relations in a lowland catchment using hydrograph fitting, recession analysis, and soil moisture data, Water Resources Research, 49, 4257–4264, https://doi.org/10.1002/wrcr.20320, http://onlinelibrary.wiley.com/doi/10.1002/wrcr.20320/abstract, 2013.

Buitink, J., Uijlenhoet, R., and Teuling, A. J.: Evaluating seasonal hydrological extremes in mesoscale (pre-)Alpine basins at coarse 0.5° and fine hyperresolution, Hydrology and Earth System Sciences Discussions, pp. 1–23, https://doi.org/https://doi.org/10.5194/hess-2018-407, https://www.hydrol-earth-syst-sci-discuss.net/hess-2018-407/, 2018.

Buitink, J., Melsen, L. A., Kirchner, J. W., and Teuling, A. J.: A distributed simple dynamical systems approach (dS2 v1.0) for computationally efficient hydrological modelling at high spatio-temporal resolution, Geoscientific Model Development, 13, 6093–6110, https://doi.org/https://doi.org/10.5194/gmd-13-6093-2020, https://gmd.copernicus.org/articles/13/6093/2020/, publisher: Copernicus GmbH, 2020.

C3S: ERA5: Fifth generation of ECMWF atmospheric reanalyses of the global climate, Copernicus Climate Change Service Climate Data Store (CDS), https://cds.climate.copernicus.eu/cdsapp#!/home, 2017.

Clapp, R. B. and Hornberger, G. M.: Empirical equations for some soil hydraulic properties, Water Resources Research, 14, 601–604, https://doi.org/10.1029/WR014i004p00601, https://agupubs.onlinelibrary.wiley.com/doi/abs/10.1029/WR014i004p00601, _eprint: https://agupubs.onlinelibrary.wiley.com/doi/pdf/10.1029/WR014i004p00601, 1978.

Collins, D. N.: Climatic warming, glacier recession and runoff from Alpine basins after the Little Ice Age maximum, Annals of Glaciology, 48, 119–124, https://doi.org/10.3189/172756408784700761, https://www.cambridge.org/core/journals/annals-of-glaciology/article/climatic-warming-glacier-recession-and-runoff-from-alpine-basins-after-the-little-ice-age-maximum/4C9795D0AF76E88C061E13F4A65BEB12/core-reader, publisher: Cambridge University Press, 2008.

Comola, F., Schaefli, B., Ronco, P. D., Botter, G., Bavay, M., Rinaldo, A., and Lehning, M.: Scale-dependent effects of solar radiation patterns on the snow-dominated hydrologic response, Geophysical Research Letters, 42, 3895–3902, https://doi.org/10.1002/2015GL064075, https://agupubs.onlinelibrary.wiley.com/doi/abs/10.1002/2015GL064075, 2015.

Cornes, R. C., van der Schrier, G., van den Besselaar, E. J. M., and Jones, P. D.: An Ensemble Version of the E-OBS Temperature and Precipitation Data Sets, Journal of Geophysical Research: Atmospheres, 123, 9391–9409, https://doi.org/10.1029/2017JD028200, https://agupubs.onlinelibrary.wiley.com/doi/full/10.1029/2017JD028200, tex.ids: cornes_ensemble_2018a number: 17, 2018.

Denissen, J. M. C., Teuling, A. J., Reichstein, M., and Orth, R.: Critical Soil Moisture Derived From Satellite Observations Over Europe, Journal of Geophysical Research: Atmospheres, 125, e2019JD031 672, https://doi.org/10.1029/2019JD031672, https://agupubs.onlinelibrary.wiley.com/doi/abs/10.1029/2019JD031672, number: 6, 2020.

Fontrodona Bach, A., Schrier, G. v. d., Melsen, L. A., Tank, A. M. G. K., and Teuling, A. J.: Widespread and Accelerated Decrease of Observed Mean and Extreme Snow Depth Over Europe, Geophysical Research Letters, 45, 12,312–12,319, https://doi.org/10.1029/2018GL079799, https://agupubs.onlinelibrary.wiley.com/doi/abs/10.1029/2018GL079799, _eprint: https://agupubs.onlinelibrary.wiley.com/doi/pdf/10.1029/2018GL079799, 2018.

Hidalgo, H. G., Das, T., Dettinger, M. D., Cayan, D. R., Pierce, D. W., Barnett, T. P., Bala, G., Mirin, A., Wood, A. W., Bonfils, C., Santer, B. D., and Nozawa, T.: Detection and Attribution of Streamflow Timing Changes to Climate Change in the Western United States, Journal of Climate, 22, 3838–3855, https://doi.org/10.1175/2009JCLI2470.1, https://journals.ametsoc.org/doi/full/10.1175/2009JCLI2470.1, publisher: American Meteorological Society, 2009.

Huntington, T. G.: Evidence for intensification of the global water cycle: Review and synthesis, Journal of Hydrology, 319, 83–95, https://doi.org/10.1016/j.jhydrol.2005.07.003, http://linkinghub.elsevier.com/retrieve/pii/S0022169405003215, 2006.

Hurkmans, R. T. W. L., Terink, W., Uijlenhoet, R., Torfs, P., Jacob, D., and Troch, P. A.: Changes in streamflow dynamics in the Rhine basin under three high-resolution regional climate scenarios, Journal of Climate, 23, 679–699, https://doi.org/10.1175/2009JCLI3066.1, http://journals.ametsoc.org/doi/abs/10.1175/2009JCLI3066.1, 2010.

Huss, M.: Present and future contribution of glacier storage change to runoff from macroscale drainage basins in Europe, Water Resources Research, 47, https://doi.org/10.1029/2010WR010299, https://agupubs.onlinelibrary.wiley.com/doi/abs/10.1029/2010WR010299, _eprint: https://agupubs.onlinelibrary.wiley.com/doi/pdf/10.1029/2010WR010299, 2011.

Huuskonen, A., Saltikoff, E., and Holleman, I.: The Operational Weather Radar Network in Europe, Bulletin of the American Meteorological Society, 95, 897–907, https://doi.org/10.1175/BAMS-D-12-00216.1, https://journals.ametsoc.org/doi/full/10.1175/BAMS-D-12-00216.1, 2013.

Immerzeel, W. W., Lutz, A. F., Andrade, M., Bahl, A., Biemans, H., Bolch, T., Hyde, S., Brumby, S., Davies, B. J., Elmore, A. C., Emmer, A., Feng, M., Fernández, A., Haritashya, U., Kargel, J. S., Koppes, M., Kraaijenbrink, P. D. A., Kulkarni, A. V., Mayewski, P. A., Nepal, S., Pacheco, P., Painter, T. H., Pellicciotti, F., Rajaram, H., Rupper, S., Sinisalo, A., Shrestha, A. B., Viviroli, D., Wada, Y., Xiao, C., Yao, T., and Baillie, J. E. M.: Importance and vulnerability of the world's water towers, Nature, 577, 364–369, https://doi.org/10.1038/s41586-019-1822-y, https://www.nature.com/articles/s41586-019-1822-y, number: 7790 Publisher: Nature Publishing Group, 2020.

Jenicek, M. and Ledvinka, O.: Importance of snowmelt contribution to seasonal runoff and summer low flows in Czechia, Hydrology and Earth System Sciences, 24, 3475–3491, https://doi.org/https://doi.org/10.5194/hess-24-3475-2020, https://hess.copernicus.org/articles/24/3475/2020/, publisher: Copernicus GmbH, 2020.

Karlsen, R. H., Bishop, K., Grabs, T., Ottosson-Löfvenius, M., Laudon, H., and Seibert, J.: The role of landscape properties, storage and evapotranspiration on variability in streamflow recessions in a boreal catchment, Journal of Hydrology, 570, 315–328, https://doi.org/10.1016/j.jhydrol.2018.12.065, http://www.sciencedirect.com/science/article/pii/S0022169419300435, 2019.

Kirchner, J. W.: Catchments as simple dynamical systems: Catchment characterization, rainfall-runoff modeling, and doing hydrology backward, Water Resources Research, 45, W02 429, https://doi.org/10.1029/2008WR006912, http://doi.wiley.com/10.1029/2008WR006912, 2009.

Kirkby, M. J.: Tests of the random network model, and its application to basin hydrology, Earth Surface Processes, 1, 197–212, https://doi.org/10.1002/esp.3290010302, https://onlinelibrary.wiley.com/doi/abs/10.1002/esp.3290010302, 1976.

Kling, H. and Gupta, H.: On the development of regionalization relationships for lumped watershed models: The impact of ignoring subbasin scale variability, Journal of Hydrology, 373, 337–351, https://doi.org/10.1016/j.jhydrol.2009.04.031, http://www.sciencedirect.com/science/article/pii/S0022169409002893, 2009.

Krier, R., Matgen, P., Goergen, K., Pfister, L., Hoffmann, L., Kirchner, J. W., Uhlenbrook, S., and Savenije, H. H. G.: Inferring catchment precipitation by doing hydrology backward: A test in 24 small and mesoscale catchments in Luxembourg, Water Resources Research, 48, W10 525, https://doi.org/10.1029/2011WR010657, http://onlinelibrary.wiley.com/doi/10.1029/2011WR010657/abstract, 2012.

Laio, F., Porporato, A., Ridolfi, L., and Rodriguez-Iturbe, I.: Plants in water-controlled ecosystems: active role in hydrologic processes and response to water stress: II. Probabilistic soil moisture dynamics, Advances in Water Resources, 24, 707–723, https://doi.org/10.1016/S0309-1708(01)00005-7, http://www.sciencedirect.com/science/article/pii/S0309170801000057, 2001.

Linde, A. H. t., Aerts, J. C. J. H., Bakker, A. M. R., and Kwadijk, J. C. J.: Simulating low-probability peak discharges for the Rhine basin using resampled climate modeling data, Water Resources Research, 46, https://doi.org/10.1029/2009WR007707, https://agupubs.onlinelibrary.wiley.com/doi/abs/10.1029/2009WR007707, _eprint: https://agupubs.onlinelibrary.wiley.com/doi/pdf/10.1029/2009WR007707, 2010.

Lobligeois, F., Andréassian, V., Perrin, C., Tabary, P., and Loumagne, C.: When does higher spatial resolution rainfall information improve streamflow simulation? An evaluation using 3620 flood events, Hydrology and Earth System Sciences, 18, 575–594, https://doi.org/10.5194/hess-18-575-2014, http://www.hydrol-earth-syst-sci.net/18/575/2014/, 2014.

Loft, R.: Earth System Modeling Must Become More Energy Efficient, Eos, https://doi.org/https://doi.org/10.1029/2020EO147051, https://doi.org/10.1029/2020EO147051, library Catalog: eos.org, 2020.

Martens, B., Miralles, D. G., Lievens, H., van der Schalie, R., de Jeu, R. A. M., Fernández-Prieto, D., Beck, H. E., Dorigo, W. A., and Verhoest, N. E. C.: GLEAM v3: satellite-based land evaporation and root-zone soil moisture, Geoscientific Model Development, 10, 1903–1925, https://doi.org/https://doi.org/10.5194/gmd-10-1903-2017, https://gmd.copernicus.org/articles/10/1903/2017/, publisher: Copernicus GmbH, 2017.

Mastrotheodoros, T., Pappas, C., Molnar, P., Burlando, P., Manoli, G., Parajka, J., Rigon, R., Szeles, B., Bottazzi, M., Hadjidoukas, P., and Fatichi, S.: More green and less blue water in the Alps during warmer summers, Nature Climate Change, 10, 155–161, https://doi.org/10.1038/s41558-019-0676-5, https://www.nature.com/articles/s41558-019-0676-5, 2020.

Melsen, L. A., Teuling, A. J., van Berkum, S. W., Torfs, P. J. J. F., and Uijlenhoet, R.: Catchments as simple dynamical systems: A case study on methods and data requirements for parameter identification, Water Resources Research, 50, 5577–5596, https://doi.org/10.1002/2013WR014720, http://onlinelibrary.wiley.com/doi/10.1002/2013WR014720/abstract, 2014.

Melsen, L. A., Teuling, A., Torfs, P., Zappa, M., Mizukami, N., Clark, M., and Uijlenhoet, R.: Representation of spatial and temporal variability in large-domain hydrological models: case study for a mesoscale pre-Alpine basin, Hydrology and Earth System Sciences, 20, 2207–2226, https://doi.org/10.5194/hess-20-2207-2016, http://www.hydrol-earth-syst-sci.net/20/2207/2016/, 2016.

Melsen, L. A., Addor, N., Mizukami, N., Newman, A. J., Torfs, P. J. J. F., Clark, M. P., Uijlenhoet, R., and Teuling, A. J.: Mapping (dis)agreement in hydrologic projections, Hydrology and Earth System Sciences, 22, 1775–1791, https://doi.org/https://doi.org/10.5194/hess-22-1775-2018, https://hess.copernicus.org/articles/22/1775/2018/, publisher: Copernicus GmbH, 2018.

Middelkoop, H., Daamen, K., Gellens, D., Grabs, W., Kwadijk, J. C., Lang, H., Parmet, B. W., Schädler, B., Schulla, J., and Wilke, K.: Impact of climate change on hydrological regimes and water resources management in the Rhine basin, Climatic Change, 49, 105–128, http://link.springer.com/article/10.1023/A:1010784727448, 2001.

Milly, P. C. D. and Dunne, K. A.: Colorado River flow dwindles as warming-driven loss of reflective snow energizes evaporation, Science, 367, 1252–1255, https://doi.org/10.1126/science.aay9187, https://science.sciencemag.org/content/367/6483/1252, publisher: American Association for the Advancement of Science Section: Report, 2020.

Monteith, J.: Evaporation and environment, Symposia of the Society for Experimental Biology, 19, 205–234, http://europepmc.org/abstract/MED/5321565, 1965.

Musselman, K. N., Clark, M. P., Liu, C., Ikeda, K., and Rasmussen, R.: Slower snowmelt in a warmer world, Nature Climate Change, 7, 214–219, https://doi.org/10.1038/nclimate3225, https://www.nature.com/articles/nclimate3225, number: 3 Publisher: Nature Publishing Group, 2017.

Osnabrugge, B. v., Weerts, A. H., and Uijlenhoet, R.: genRE: A Method to Extend Gridded Precipitation Climatology Data Sets in Near Real-Time for Hydrological Forecasting Purposes, Water Resources Research, 53, 9284–9303, https://doi.org/10.1002/2017WR021201, https://agupubs.onlinelibrary.wiley.com/doi/abs/10.1002/2017WR021201, 2017.

Pfister, L., Kwadijk, J., Musy, A., Bronstert, A., and Hoffmann, L.: Climate change, land use change and runoff prediction in the Rhine–Meuse basins, River Research and Applications, 20, 229–241, https://doi.org/10.1002/rra.775, http://doi.wiley.com/10.1002/rra.775, 2004.

Rottler, E., Francke, T., Bürger, G., and Bronstert, A.: Long-term changes in central European river discharge for 1869–2016: impact of changing snow covers, reservoir constructions and an intensified hydrological cycle, Hydrology and Earth System Sciences, 24, 1721–1740, https://doi.org/https://doi.org/10.5194/hess-24-1721-2020, https://www.hydrol-earth-syst-sci.net/24/1721/2020/, publisher: Copernicus GmbH, 2020.

Ruiz-Villanueva, V., Borga, M., Zoccatelli, D., Marchi, L., Gaume, E., and Ehret, U.: Extreme flood response to short-duration convective rainfall in South-West Germany, Hydrology and Earth System Sciences, 16, 1543–1559, https://doi.org/https://doi.org/10.5194/hess-16-1543-2012, https://www.hydrol-earth-syst-sci.net/16/1543/2012/hess-16-1543-2012.html, 2012.

Rupp, D. E. and Selker, J. S.: On the use of the Boussinesq equation for interpreting recession hydrographs from sloping aquifers, Water Resources Research, 42, W12 421, https://doi.org/10.1029/2006WR005080, https://agupubs.onlinelibrary.wiley.com/doi/abs/10.1029/2006WR005080, 2006.

Seneviratne, S. I., Lehner, I., Gurtz, J., Teuling, A. J., Lang, H., Moser, U., Grebner, D., Menzel, L., Schroff, K., Vitvar, T., and Zappa, M.: Swiss prealpine Rietholzbach research catchment and lysimeter: 32 year time series and 2003 drought event, Water Resources Research, 48, W06 526, https://doi.org/10.1029/2011WR011749, http://onlinelibrary.wiley.com/doi/10.1029/2011WR011749/abstract, 2012.

Settele, J., Scholes, R., Betts, R., Bunn, S., Leadley, P., Nepstad, D., Overpeck, J., Taboada, M., Fischlin, A., Moreno, J., Root, T., Musche, M., and Winter, M.: Terrestrial and Inland water systems, in: Climate Change 2014 Impacts, Adaptation and Vulnerability: Part A: Global and Sectoral Aspects, pp. 271–360, https://doi.org/10.1017/CBO9781107415379.009, 2015.

Shabalova, M. V., van Deursen, W. P. A., and Buishand, T. A.: Assessing future discharge of the river Rhine using regional climate model integrations and a hydrological model, Climate Research, 23, 233–246, http://www.int-res.com/abstracts/cr/v23/n3/p233-246/, 2003.

Stahl, K., Weiler, M., Kohn, I., Freudiger, D., Seibert, J., Vis, M., Gerlinger, K., and Bohm, M.: The snow and glacier melt components of streamflow of the river Rhine and its tributaries considering the influence climate change, Tech. Rep. I-25, CHR, http://www.chr-khr.org/sites/default/files/chrpublications/asg-rhein_synthesis_en.pdf, 2016.

Stocker, T. F., Qin, D., Plattner, G. K., Tignor, M., Allen, S. K., Boschung, J., Nauels, A., Xia, Y., Bex, B., and Midgley, B. M.: IPCC, 2013: Climate Change 2013: The physical science basis. Contribution of Working Group I to the Fifth Assessment report of the Intergovernmental Panel on Climate Change, 2013.

Takala, M., Pulliainen, J., Metsamaki, S. J., and Koskinen, J. T.: Detection of snowmelt using spaceborne microwave radiometer data in Eurasia from 1979 to 2007, IEEE Transactions on Geoscience and Remote Sensing, 47, 2996–3007, publisher: IEEE, 2009.

Tank, A. M. G. K., Wijngaard, J. B., Können, G. P., Böhm, R., Demarée, G., Gocheva, A., Mileta, M., Pashiardis, S., Hejkrlik, L., Kern-Hansen, C., Heino, R., Bessemoulin, P., Müller-Westermeier, G., Tzanakou, M., Szalai, S., Pálsdóttir, T., Fitzgerald, D., Rubin, S., Capaldo, M., Maugeri, M., Leitass, A., Bukantis, A., Aberfeld, R., Engelen, A. F. V. v., Forland, E., Mietus, M., Coelho, F., Mares, C., Razuvaev, V., Nieplova, E., Cegnar, T., López, J. A., Dahlström, B., Moberg, A., Kirchhofer, W., Ceylan, A., Pachaliuk, O., Alexander, L. V., and Petrovic, P.: Daily dataset of 20th-century surface air temperature and precipitation series for the European Climate Assessment, International Journal of Climatology, 22, 1441–1453, https://doi.org/https://doi.org/10.1002/joc.773, https://rmets.onlinelibrary.wiley.com/doi/abs/10.1002/joc.773, _eprint: https://rmets.onlinelibrary.wiley.com/doi/pdf/10.1002/joc.773, 2002.

Teuling, A. J., Lehner, I., Kirchner, J. W., and Seneviratne, S. I.: Catchments as simple dynamical systems: Experience from a Swiss prealpine catchment, Water Resources Research, 46, W10 502, https://doi.org/10.1029/2009WR008777, http://doi.wiley.com/10.1029/2009WR008777, 2010.

Teuling, A. J., Badts, E. A. G. d., Jansen, F. A., Fuchs, R., Buitink, J., Hoek van Dijke, A. J., and Sterling, S. M.: Climate change, reforestation/afforestation, and urbanization impacts on evapotranspiration and streamflow in Europe, Hydrology and Earth System Sciences, 23, 3631–3652, https://doi.org/https://doi.org/10.5194/hess-23-3631-2019, https://www.hydrol-earth-syst-sci.net/23/3631/2019/, publisher: Copernicus GmbH, 2019.

Tóth, B., Weynants, M., Pásztor, L., and Hengl, T.: 3D soil hydraulic database of Europe at 250 m resolution, Hydrological Processes, 31, 2662–2666, https://doi.org/10.1002/hyp.11203, https://onlinelibrary.wiley.com/doi/abs/10.1002/hyp.11203, _eprint: https://onlinelibrary.wiley.com/doi/pdf/10.1002/hyp.11203, 2017.

Wang, K., Dickinson, R. E., Wild, M., and Liang, S.: Evidence for decadal variation in global terrestrial evapotranspiration between 1982 and 2002: 2. Results, Journal of Geophysical Research: Atmospheres, 115, https://doi.org/10.1029/2010JD013847, https://agupubs.onlinelibrary.wiley.com/doi/abs/10.1029/2010JD013847, _eprint: https://agupubs.onlinelibrary.wiley.com/doi/pdf/10.1029/2010JD013847, 2010.

Wild, M., Folini, D., Schär, C., Loeb, N., Dutton, E. G., and König-Langlo, G.: The global energy balance from a surface perspective, Climate Dynamics, 40, 3107–3134, https://doi.org/10.1007/s00382-012-1569-8, https://link.springer.com/article/10.1007/s00382-012-1569-8, 2013.